Contents

1 Topological materials

In this chapter, we consider various concepts from physics that are relevant in the context of topological materials. Firstly, the symmetry related concepts of parity, time reversal, Kramer's degeneracy, and accidental degeneracy are explained. Then, the concept of linear dispersion in Weyl and Dirac cones is discussed, along with some useful results. Lastly follows a quick summary of spin-orbit interactions. The chapter is intended as a quick introduction to the vast field of topological materials for someone who are not familiar with these concepts.

Some topics discussed are directly applicable to the thesis, while others are included both in order to put the concepts of the thesis in a greater context, and also with regards to further continuation of this work.

1.1 Parity

We consider now the discrete transformation of space inversion, or *parity*. Firstly, basic properties of the transformation will be presented and discussed. Its effect on the position, momentum, and angular momentum operators will be discussed, before a more general discussion on how it transforms proper- and pseudo-tensors. This will be applied to see how the parity transformation affects electric and magnetic fields.

Let the parity operator P be a unitary operator

$$P: \quad |a\rangle \to P\,|a\rangle\,. \tag{1.1}$$

By definition, we require

$$P^\dagger x P = -x, \tag{1.2}$$

$$P^\dagger p P = -p, \tag{1.3}$$

where x, p are the position and momentum operators. By the unitarity of P, which means that $P^\dagger P = I$,

$$xP = -Px.$$

We now use this anticommutation to find an explicit form of the transformation in the position representation. By noting that, given the position eigenstate $|x_1\rangle$,

$$xP\,|x_1\rangle = -Px_1\,|x_1\rangle = -x_1P\,|x_1\rangle\,, \tag{1.4}$$

with x_1 the eigenvalue of the state, we may conclude

$$P\,|x_1\rangle = |-x_1\rangle$$

up to some arbitrary phase. We chose this phase to be unity. Then

$$P^2\,|x_1\rangle = |x_1\rangle \tag{1.5}$$

for any position eigenstate, which gives the operator relation $P^2 = 1 \implies P = \pm 1$. This also means that P is Hermitian,

$$P = P^{-1} = P^\dagger.$$

The treatment of angular momentum is somewhat more involved. Some sources simply state that as the orbital angular momentum

$$L = x \times p$$

is a product of two odd quantities, it must be even under parity. This, of course, is a gross over simplification, as extra care must be taken when considering the spin angular momentum S contributing to the total angular momentum

$$J = L + S.$$

The angular momentum operator is the generator of rotations

$$R = e^{-i\epsilon J\cdot n} \approx 1 - i\epsilon J \cdot n$$

where we expanded the operator under the assumption of a small angle, $\epsilon \ll 1$. As rotations are invariant during space inversion,

$$P^\dagger RP = R \tag{1.6}$$

$$\implies P^\dagger J \cdot nP = J \cdot n \tag{1.7}$$

from which it follows that

$$P^\dagger JP = J, \tag{1.8}$$

as the parity operator obviously does not act on the normal vector n. Thus, the angular momentum operator, unlike the linear momentum operator, is even under parity.

For a general vector-like[1] quantity V, we will consider how it transforms during space inversion. If the quantity "flips" during space inversion, $P^\dagger V P = -V$, we say simply that it is a vector, also sometimes known as a polar vector. Quantities that do not "flip", so that they turn into their opposites in the flipped image, we denote pseudo vectors. Thus, depending on whether the eigenvalue of an operator under space inversion is $+1$ or -1 we say that it is either a pseudo-vector or vector, respectively. Position and momentum are examples of vectors, while angular momentum and the magnetic field are examples of pseudo-vectors. An illustrative explanation of this is shown in Figure 1.1, which explains both angular momentum and magnetic fields.

Remark about dimensionality: The above discussion about parity, which is the standard way to present parity in condensed matter physics, is valid for three dimensions. In two dimensions, however, one must separate *parity* and *space inversion*. The former takes a right-handed system to a left-handed system [13], while the latter inverts space, $\boldsymbol{x} \to -\boldsymbol{x}$. In odd dimensions this is the same, while in even dimensions they differ. In even dimensions, inversion corresponds to a rotation, while a parity transform is different from any rotation. In more formal terms, inversion is part of the group of proper rotations $SO(n)$ for even dimensions, as the determinant is $+1$, the definition of a proper rotation. Parity should in general be taken to be the operation P such that the group of all rotations $O(n) = SO(n) \times \{E, P\}$, with E the identity transformation. This will not be of direct importance here, but it is an important detail to note.

1.2 Time reversal

We will now consider the time reversal operator Θ. Firstly we will show that it must be antiunitary, then we will show $\Theta^2 = \pm 1$, and find a more specific form of Θ for half-integer spin systems.

The time reversal operator by definition will invert the value of the time

$$\Theta : t \to -t$$

while leaving space unchanged. The invariance of space is summaries by the operator relation,

$$\Theta x \Theta^{-1} = x, \tag{1.9}$$

[1]We use the term *vector-like* instead of vector, as the term vector is defined as something that is odd under parity, as opposed to for example a pseudo vector, even though they naively "look" like vectors. This can be compared to tensors. The definition of a tensor is something that transforms like a tensor under a Lorentz transformation, so we may have matrix objects that "look" like tensors, but transforms differently.

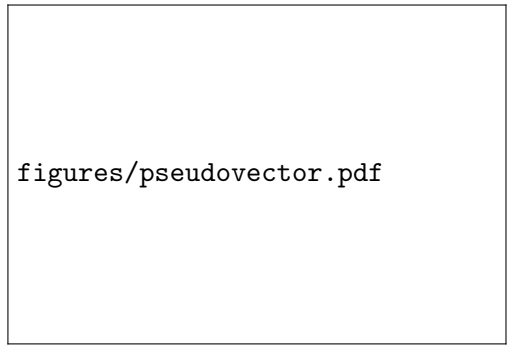

Figure 1.1: Schematic illustration of vectors and pseudovectors. A vector field with curl, which may be taken to be either momentum or current, is shown as a rotating arrow. The curl of this field, which will respectively be the angular momentum or B-field, is shown as a straight arrow. Under inversion, shown as a mirror operation, the curl generated by the field is inverted in addition to the mirroring, i.e. rotated. This non-formal illustration gives an intuitive explanation of the concepts vector and pseudovector. Note that as the example is two-dimensional, mirror symmetry here the same as parity, and not inversion. See main text for details.

where x is understood as the position operator. The momentum operator, however, is flipped due to its time dependence

$$\Theta p \Theta^{-1} = -p. \tag{1.10}$$

A schematic representation of inversion symmetry and time reversal symmetry is given in Figure 1.2.

We are now in a position to show that Θ must be antiunitary by requiring the invariance of the commutation relation between momentum and position, $[x, p] = i\hbar$.

$$\Theta[x, p]\Theta^{-1} = \Theta i\hbar\Theta^{-1} = -[x, p] = -i\hbar. \tag{1.11}$$

In the first equality, the commutation relation was used directly. In the second equality, Eqs. (1.9) and (1.10) were used to gain a minus sign. This all leads to the relation

$$\Theta i \Theta^{-1} = -i. \tag{1.12}$$

From this, we gather that the time reversal operator must be antiunitary. An antiunitary transformation is a transformation

$$|a\rangle \to |\tilde{a}\rangle = \theta\,|a\rangle\,, \quad |b\rangle \to |\tilde{b}\rangle = \theta\,|b\rangle\,,$$

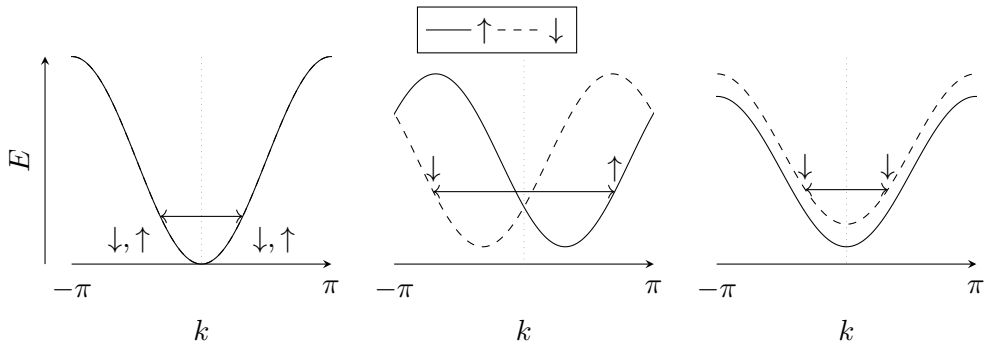

Figure 1.2: Schematic illustration of time and inversion breaking of degenerate energy bands of a two-level system. The two levels are denoted ↑ and ↓. **(Left:)** Both time-reversal and inversion symmetry present, with the two energy bands being degenerate at all momenta. **(Center:)** Inversion symmetry is broken. Notice how at the TRIM (time reversal independent momenta) points, $-\pi, 0, \pi$, the two energy levels are degenerate, as, by definition, we have $\boldsymbol{k} = -\boldsymbol{k}$. **(Right:)** Time reversal symmetry is broken. Notice how in the time reversal symmetric case Kramer's doublet is present, as for any state at k, the state at $-k$ is degenerate in energy and has opposite spin. This is not the case when time reversal symmetry is broken, as the spin at $-k$ has the same spin. Figure inspired by Ramazashvili [12].

such that

$$\langle \tilde{b} | \tilde{a} \rangle = \langle b | a \rangle^* , \tag{1.13}$$

$$\theta \left(c_1 \left| a \right\rangle + c_2 \left| b \right\rangle \right) = c_1^* \theta \left| a \right\rangle + c_2^* \theta \left| b \right\rangle . \tag{1.14}$$

A note of caution: the Dirac bra-ket notation was originally designed to handle linear operators, where it excels. For anti-linear operators, which antiunitary operators are, the bra-ket notation can be deceiving. We will always take anti-linear operators to work on kets, never on bras from the right. So, for example,

$$\langle a | O | b \rangle$$

should be understood as

$$\langle a | \left(| O | b \rangle \right)$$

and *never*

$$\left(\langle a | O | \right) | b \rangle .$$

The left operation of an anti-linear operator on a bra, $\langle a| O$, will not be defined.

We will in general write

$$\Theta = UK \tag{1.15}$$

where U is a unitary transformation and K is the complex conjugation. Now, we will show that $\Theta^2 = \pm 1$, by an elegant method inspired by Bernevig and Hughes [2]. Consider

$$\Theta^2 = UKUK = UU^* = U(U^T)^{-1} \equiv \phi, \tag{1.16}$$

where we in the second last equality used the unitarity of U. As applying the time reversal operator twice must result in the original state, up to some phase, ϕ must surely be diagonal. From Eq. (1.16) it follows

$$U = \phi U^T, \quad U^T = U\phi \tag{1.17}$$

where the fact that $\phi^T = \phi$ for any diagonal matrix was used. From this follows that

$$U = \phi U \phi \Rightarrow U\phi^{-1} = \phi U. \tag{1.18}$$

This holds in general only for $\phi = \pm 1$, and thus $\Theta^2 = \pm 1$. Furthermore, we will later show that for integer spin particles $\Theta^2 = 1$ while for half-integer spin particles $\Theta^2 = -1$.

1.2.1 Time reversal operator on spinful particles

When considering spinful particles, we must enforce yet another property on the time reversal operator. As spin is odd under time reversal one must have

$$\Theta S \Theta^{-1} = -S. \tag{1.19}$$

Consider now specifically a spin-s state, with the basis $|s, m\rangle$, being an eigenstate of $S_z, \boldsymbol{S}^2$, with eigenvalues $m\hbar, s(s+1)\hbar^2$ respectively. By Eq. (1.19) it follows that $\Theta |s, m\rangle$ is also an eigenstate of S_z, with eigenvalue $-m\hbar$, since

$$S_z \Theta |s, m\rangle = -\Theta S_z |s, m\rangle = -m\hbar\Theta |s, m\rangle . \tag{1.20}$$

Let

$$\Theta |s, m\rangle = \eta |s, -m\rangle ,$$

where η is some phase. Consider now the commutation of the ladder operators $J_\pm = S_x \pm iS_y$ with the time reversal operator.

$$\begin{aligned} \underbrace{[S_x \pm iS_y]}_{S_\pm} \Theta &= -\Theta S_x \mp i\Theta S_y \\ &= -\Theta \underbrace{[S_x \mp iS_y]}_{S_\mp}, \end{aligned} \tag{1.21}$$

where the anti-linearity of Θ is emphasized. Thus, operating with S_+ on $\Theta\,|s,m\rangle$ gives

$$S_+\Theta\,|s,m\rangle = \eta_{sm}S_+\,|s,-m\rangle \tag{1.22}$$
$$= \eta_{sm}\hbar\sqrt{(s+m)(s-m+1)}\,|s,-m+1\rangle\,. \tag{1.23}$$

On the other hand, commuting the two operators first gives

$$S_+\Theta\,|s,m\rangle = -\Theta S_-\,|s,m\rangle \tag{1.24}$$
$$= -\Theta\hbar\sqrt{(s+m)(s-m+1)}\,|s,m-1\rangle \tag{1.25}$$
$$= -\hbar\sqrt{(s+m)(s-m+1)}\eta_{s,m-1}\,|s,-m+1\rangle\,. \tag{1.26}$$

By comparison, $\eta_{sm} = -\eta_{s,m-1}$; η_{sm} has a flip of its sign under increments of m. The m dependence should therefore be $(-1)^m$. For later convenience, we will choose to also include an s-term in the exponent, so that the exponent is integer also for half-integer systems, resulting in

$$\eta_{sm} = (-1)^{s-m}f(s), \tag{1.27}$$

where $f(s)$ is some phase that does not depend on m. We are now in a position where we may find Θ^2, by acting on a general spin s system.

$$\Theta^2\sum_{m=-s}^{s}a_m\,|s,m\rangle = \Theta\sum_m a_m^* f(s)(-1)^{s-m}\,|s,-m\rangle \tag{1.28}$$
$$= \sum_m a_m f^*(s)(-1)^{s-m}\Theta\,|s,-m\rangle \tag{1.29}$$
$$= \sum_m a_m|f(s)|^2(-1)^{2s}\,|s,m\rangle\,. \tag{1.30}$$

Note that it was important that $(-1)^{s-m}$ was real, which is taken care of by the s-term. As $f(s)$ is only a phase, this gives

$$\Theta^2 = (-1)^{2s}, \tag{1.31}$$

for any spin s system. Thus, for half integer spin, $\frac{1}{2}, \frac{3}{2}, \ldots$, $\Theta^2 = -1$, while for integer spin $\Theta^2 = +1$.

1.3 Kramer's degeneracy

Kramer's degeneracy states that for any half-integer system that is time-reversal symmetric, energy levels are at least two-fold degenerate. The proof of this is

simple, and uses the fact that for any half-integer spin system, $\Theta^2 = -1$. A heuristic way to see this is the fact that spin is odd under time-reversal, and for half-integer systems there is no zero-spin state, so reversing the spin cannot result in the same state.

Proof: Assume

$$[H, \Theta] = 0$$

and that $|n\rangle$ is an eigenstate of the system

$$H|n\rangle = E_n|n\rangle .$$

Then

$$H\Theta|n\rangle = \Theta H|n\rangle = \Theta E_n|n\rangle = E_n\Theta|n\rangle$$

and so $\Theta|n\rangle$ is also an eigenstate with the eigenvalue E_n. To assert that the eigenvalue is in fact degenerate, one must also show that the two states are not the same ray. That is $\Theta|n\rangle \neq e^{i\delta}|n\rangle$, where δ is some phase. Suppose that the above is *not* true, $\Theta|n\rangle = e^{i\delta}|n\rangle$. Then,

$$\Theta^2|n\rangle = \Theta e^{i\delta}|n\rangle = e^{-i\delta}\Theta|n\rangle = +|n\rangle .$$

However, as was stated above, $\Theta^2 = -1$ for all half-integer systems. The assumption must therefore be wrong, and the eigenvalue is degenerate. □

The two states, $|n\rangle$ and $\Theta|n\rangle$, are often referred to as Kramer's doublet. Note that the two states have opposite spin.

1.3.1 Generalization to the $P\Theta$ operator

Consider now a time reversal and parity symmetric system, $[H, P\Theta] = 0$. This will, similarly to the case for time reversal, make the energy levels at least two-fold degenerate.

Proof: Assume

$$[H, P\Theta] = 0$$

and that $|n\rangle$ is an eigenstate of the system

$$H|n\rangle = E_n|n\rangle .$$

Then

$$HP\Theta|n\rangle = P\Theta H|n\rangle = P\Theta E_n|n\rangle = E_nP\Theta|n\rangle .$$

Assume now that $P\Theta |n\rangle = e^{i\delta} |n\rangle$, which we will prove to be false. That would lead to

$$(P\Theta)^2 |n\rangle = P\Theta e^{i\delta} |n\rangle = |n\rangle .$$

However, as $[P, \Theta] = 0$, we have

$$(P\Theta)^2 = P\Theta P\Theta = P\Theta^2 P = -1$$

as $P^2 = 1$. As above, the states are thus different, and the eigenvalue is degenerate. □

1.4 Accidental degeneracy

In general, for a two level system depending on some parameter the energy levels of the two levels will not cross, i.e. be degenerate, unless there are symmetries in the system forcing them to be degenerate, as is the case in for example Kramer's degeneracy. However, even without any symmetries [2] there will be so-called *accidental degeneracies* if the parameter space is sufficiently large. Consider a general two-level Hamiltonian

$$H = f_1\sigma_x + f_2\sigma_y + f_3\sigma_z, \tag{1.32}$$

which will have an energy splitting between the two levels

$$\Delta E = 2\sqrt{f_1^2 + f_2^2 + f_3^2}. \tag{1.33}$$

In general, we may solve $\Delta E = 0$ by tuning the three parameters simultaneously, and thus there must be degenerate points – accidental degeneracies. Supposing that the parameters f_i can be expressed as functions of the momentum components, $f_i = f_i(p_i)$, this will correspond to degenerate points in momentum space.

If there are in addition some symmetry constraints on the system, the space of degenerate points may increase. Suppose, for example, the system is time reversal symmetric. Recalling the time reversal operator defined in Eq. (1.15)

$$\Theta = UK,$$

with U being a unitary operator and K the complex conjugate, the imaginary Pauli matrix σ_y must be excluded. Thus, the solution to the closing of the band gap has a free parameter, and the degenerate space has dimension one.

[2] There will always, for a degenerate system, be some symmetry, although it might be a *hidden* symmetry. We here mean no a priori apparent symmetry.

1.5 Spin-orbit interaction

Spin-orbit interactions are not used directly in this thesis. It is, however, relevant to include some superficial introduction to the subject, both in order to conclude that spin-orbit interactions are not something one has to consider in later derivations of this thesis, and also that it might prove useful in future applications of the ideas and theory discussed in the thesis.

Spin-1/2 particles are in general governed by the Dirac equation. In the non-relativistic regime, as is the case in condensed matter physics, we may reduce the equation to the Pauli equation. This equation contains as a relativistic correction the spin orbit coupling term [5]

$$H_{SO} = \lambda_{\text{vac}} \boldsymbol{\sigma} \cdot (\boldsymbol{k} \times \nabla \tilde{V}), \tag{1.34}$$

where λ_{vac} is a constant with dimension length squared, $\boldsymbol{\sigma}$ are the Pauli matrices representing spin, and $\tilde{V}$ is the total potential in the system. In preparation of the considerations to come, split up the potential in the periodic crystal potential V_{cr} and the remaining potential V from impurities

$$\tilde{V} = V_{\text{cr}} + V. \tag{1.35}$$

Should this be the Bloch basis

Changing basis to a quasi-particle picture of free particles, thus eliminating V_{cr} from the equation, one gets the effective Hamiltonian [5]

$$H_{\text{eff}} = \epsilon_k + V + H_{\text{int}} + H_{\text{ext}}, \tag{1.36}$$

$$H_{\text{int}} = -\frac{1}{2} \boldsymbol{b}(\boldsymbol{k}) \cdot \boldsymbol{\sigma}, \tag{1.37}$$

$$H_{\text{ext}} = \lambda \boldsymbol{\sigma} \cdot (\boldsymbol{k} \times \nabla V). \tag{1.38}$$

Here, the subscripts denote the effective Hamiltonian H_{eff}, consisting of an intrinsic part, H_{int}, and an extrinsic part, H_{ext}. $\boldsymbol{b}(\boldsymbol{k})$ is the intrinsic spin-orbit field, the part of the crystal potential V_{cr} that is not eliminated by our change of basis. As the intrinsic spin-orbit interaction should be time reversal invariant, we can argue that $\boldsymbol{b}$ must be an odd function.

$$\Theta H_{\text{int}} \Theta^{-1} = H_{\text{int}} \implies \boldsymbol{b}(\boldsymbol{k}) \cdot \boldsymbol{\sigma} = -\boldsymbol{b}(-\boldsymbol{k}) \cdot \boldsymbol{\sigma}, \tag{1.39}$$

where the well known effects of the time reversal operator was applied to the momentum and spin, as $\Theta \boldsymbol{k} \Theta^{-1} = -\boldsymbol{k}$ and $\Theta \boldsymbol{\sigma} \Theta^{-1} = -\boldsymbol{\sigma}$. Obviously, this

means that inversion symmetry must be broken for the intrinsic interaction term to be finite. This is easily seen as, with P being the parity operator,

$$PH_{\text{int}}P^{-1} = H_{\text{int}} \Rightarrow \boldsymbol{b}(-\boldsymbol{k}) = \boldsymbol{b}(\boldsymbol{k}), \tag{1.40}$$

since spin is invariant under inversion.

The external contribution to the spin-orbit interaction is contained in H_{ext}, which does not require any particular symmetry to be present. A Zeeman term, where time reversal is broken, would be represented in the external part of the Hamiltonian.

The spin-orbit field $\boldsymbol{b}(\boldsymbol{k})$ may take many forms depending on the specifics of the system at hand. The Dresselhaus term

$$H_D = \alpha p_x(p_y^2 - p_z^2)\sigma_x + \text{c.p.} \tag{1.41}$$

where c.p. denotes terms of circular permutation of the indices, [9] and the Rashba term [17]

$$H_R = \alpha(p_y\sigma_x - p_x\sigma_y), \tag{1.42}$$

are arguably the most well-known models.

We immediately see that the Rashba Hamiltonina (1.42) does not break time reversal invariance, as both momentum and spin are odd under time reversal. It is however odd under inversion. This is of course exactly opposite of a Zeeman term, where we introduce an external magnetic field, thus breaking time reversal symmetry. Consider a free electron model where we add a Rashba term

$$H = \frac{p^2}{2m} + \alpha(p_y\sigma_x - p_x\sigma_y). \tag{1.43}$$

The Hamiltonian commutes with the momentum operator, so we may replace the momentum operator with its eigenvalue $\hbar k$. Solving for the eigenvalue is straight forward, and gives

$$E_\pm = \frac{\hbar k^2}{2m} \pm \alpha k, \tag{1.44}$$

where $k = |\boldsymbol{k}|$. We expect the eigenvalues to be linear combinations of spin up and spin down states, and also that the coefficients depend on k, as the Rashba term has copuled spin and momentum. Take

$$\psi_\pm = \frac{e^{i\boldsymbol{kr}}}{\sqrt{2}}\left(|\uparrow\rangle + b\,|\downarrow\rangle\right), \tag{1.45}$$

where b is some phase we must find. By inserting into the time-independent Schrödinger equation, we find $b = \mp i(k_x + k_y)/k$, which is obviously $b =$

$\mp i \exp(i\theta)$, where θ is the angle of the momentum, $\boldsymbol{k} = (k\cos\theta, k\sin\theta)$. Using the matrix representation $|\uparrow\rangle = (1,0)^T, |\downarrow\rangle = (0,1)^T$, the eigenvalues are given as

$$\psi_\pm = \frac{e^{i\boldsymbol{kr}}}{\sqrt{2}} \begin{pmatrix} 1 \\ \mp i e^{i\theta} \end{pmatrix}. \tag{1.46}$$

These states have interesting spin expectation values

$$\langle \psi_\pm | \boldsymbol{\sigma} | \psi_\pm \rangle = \pm \left[\sin\theta \hat{x} - \cos\theta \hat{y} \right]. \tag{1.47}$$

The spin is orthogonal to the momentum, making a circular pattern around the origin. The direction of the rotation defines the chirality of the state. The spin together with the energy solutions are shown in Figure 1.3.

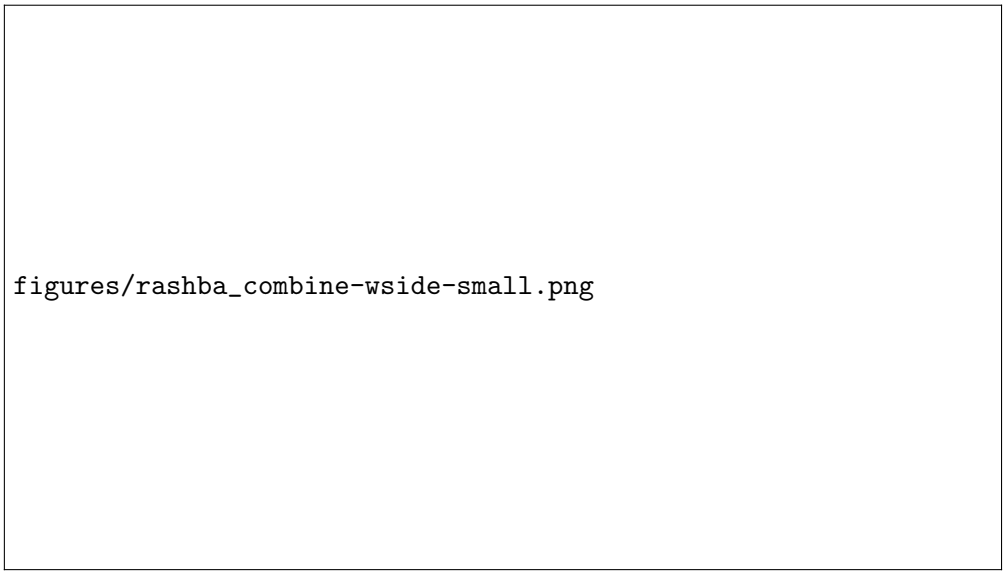

Figure 1.3: Dispersion curves for a system with Rashba spin-orbit coupling. **Left:** Seen from above. **Right:** Seen from the front. The projection into the xy-plane is shown, as well as a cross section in a plane perpendicular to the xy-plane. The spin of the two states are shown as arrow above the dispersion curves, which defines the chirality of each state. Notice, as is most easily seen in the projection, that the two solutions together form a pair of parabolas separated in momentum.

1.6 Weyl and Dirac cones in condensed matter physics

Dirac and Weyl cones are the emergence of non-gapped linear energy bands in condensed matter physics, in effect exhibiting relativistic behavior at non-relativistic speeds. We here give a very brief introduction to these materials. Firstly, we will consider the so-called band crossing, and how the opening of a gap at the band crossing behaves differently in two and three dimensions. Then, various perturbations that do not open a gap will be considered, giving interesting effects in the dispersion relations. Lastly, a consideration of these materials in light of Berry curvature and the topological quantity of Chern numbers will be given.

The standard model for metals in condensed matter physics is the Landau Fermi liquid [8; 4], where electrons are described by the Hamiltonian $p^2/2m*$, with $m*$ some effective mass. This model, however, fails for Dirac materials, where the electrons behave as "Dirac fermions". The notion of a "Dirac fermion" is almost comical from a high energy point of view[4; 16] – what else can they be? A fermion is by its very definition a Dirac spinor. In condensed matter language, however, we mean by fermion that it obeys the Pauli exclusion principle and follows the Fermi-Dirac distribution function. By Dirac fermion in condensed matter we mean fermions whose effective Hamiltonian is linear in momenta, they obey an effective Dirac equation.

This field unifies concepts from high and low energy physics; a "new era of grand unification of low and high energy phiscs" as Chernodub et al. [4] puts it. The emergent Dirac and Weyl cones in condensed matter physics follow in beautiful analogy their high energy counterparts. Thus, the theory and results form high energy physics may be applied in these emergent Dirac systems. Likewise, these materials offer the opportunity to probe the fundamental theories of our universe, and beyond, at much lower energy and cost scales. Unfortunately, some concepts of QFT and high energy physics are somewhat inaccessible for condensed matter physicists. At the same time, the condensed matter description have been difficult to relate back to the QFT formalism. So while the intersection of the two fields offer the possibility of great new insight, it also comes with some misunderstandings. Some phenomena are known under different names, while different phenomena may be mistaken for the same. The recent and excellent review paper by Chernodub et al. [4] attempts to make the topics approachable for researchers from both fields, whose "main purpose [...] is to present the basic notions underlying new developments in condensed matter in a language equally accessible to both high energy and condensed matter communities".

We wish here to briefly illuminate the connection between the high energy Dirac theory and the Dirac and Weyl semimetals of condensed matter physics,

assuming the reader to be an expert in neither. The (massive) Dirac equation reads

$$(i\partial\!\!\!/ - m)\psi = 0, \tag{1.48}$$

where $\partial\!\!\!/ = \gamma^\mu \partial_\mu$, γ^μ the gamma matrices [3], m is some mass parameter, and ψ the Dirac spinor. The systems is 4×4. The great insight of Dirac, was that the momentum and time operators had to appear at the same order, due to the requirement of Lorentz invariance. It may of course be written as the Schrodinger equation[4] $i\partial_t \psi = H\psi$, with $H = \gamma^0 m + \gamma^0 \gamma^i p_i$. Shortly after Dirac published his theory, Weyl commented that for a massless particle, the equation could be decomposed into two 2×2 equations – a Weyl decomposition. This yields two independent subsystems, themselves also linear in momentum,

$$H_\pm = \pm \boldsymbol{\sigma} \cdot \boldsymbol{p}, \tag{1.49}$$

with the $\pm$ defining the *chirality*.

Interestingly, massless Dirac fermions may appear in condensed matter as low energy effective descriptions of electronic systems near a two-band crossing. Instead of obeying the Landau Fermi liquid theory, as most materials, they obey a Dirac equation, with the speed of light being replaced by the Fermi velocity v_F. As in the high energy case, the Dirac equation may be decomposed into chiral Weyl equations

$$H_D = s v_F \boldsymbol{\sigma} \boldsymbol{p}, \tag{1.50}$$

where $\boldsymbol{\sigma}$ are the Pauli matricies, v_F the Fermi velocity, $\boldsymbol{p}$ the momentum, and $s = \pm 1$ denotes the chirality. It is here important to note that the Pauli matrices represent either real spin degree of freedom or some pseudo spin degree of freedom. Examples of pseudo spin is that of bipartite lattices, such as Graphene, in which case one must be careful when for example applying time reversal, as only real spin is odd under this operation, and not pseudo spin.

These linear low energy emergent systems may appear in both 2D and 3D. There are, however, important differences depending on the dimensionality. When we here refer to Dirac and Weyl materials, we always mean 3D systems, which has become the norm in the literature. In some older literature, the term might also be applied to 2D systems, sucha as Graphene.

The dispersion of the Hamiltonian (1.50) has a band crossing at $\boldsymbol{p} = 0$. For the two-dimensional case, a perturbation on the form $m\sigma_z$, with m some parameter, can open up a gap in the dispersion relation. This is easily verified by writing

[3] Also known as the Dirac matrices. They are any irreducible matrix representation of the Clifford algebra.

out the Hamiltonian and solving the eigenproblem

$$H_D^{(2D)} = sv_F(p_x\sigma_x + p_y\sigma_y) + m\sigma_z. \tag{1.51}$$

$$\left|H_D^{(2D)} - E\right| = 0. \tag{1.52}$$

As the Hamiltonian commutes with the momentum operator, we replace the momentum operator with its eigenvalues

$$E = \pm v_F\hbar\sqrt{k_x^2 + k_y^2 + \frac{m^2}{\hbar^2 v_F^2}}. \tag{1.53}$$

There are no solutions k_x, k_y making the energy levels degenerate. The crossing is thus only protected by symmetry considerations, and is not *topologically protected*.

In three dimensions the situation is somewhat different, with the Hamiltonian

$$H_D^{(3D)} = sv_F(p_x\sigma_x + p_y\sigma_y + p_z\sigma_z). \tag{1.54}$$

In this case, no perturbing term may open a gap at the crossing. There is no 2×2 matrix σ_4 that anticommutes with the Pauli matricies and also is linearly independent, i.e. there is no "fourth" Pauli matrix, and thus no perturbative term will open the gap. Say for example we add a term like $m\sigma_z$, where the z-direction was chosen arbitrarily. The only effect this will have on the crossing is to translate it in p_z. Tying this back to the accidental degeneracy, we see that no matter the perturbation, the three-dimensional momentum space will always have a point of degeneracy, i.e., a crossing. The crossing is *topologically protected*. A more formal approach to topological materials, is that of topological invariants – numbers related to the topology of the material. Having a non-trivial topological invariant number, is the very definition of topological materials, and we will in subsection 1.6.1 show that Dirac cones makes the Chern number of these materials non-trivial.

Opposed to high energy physics, the emergent Dirac equation in condensed matter physics need of course not be Lorentz invariant. We may therefore introduce terms that break Lorentz invariance. Introduce to the system a pseudospin degree of freedom, thus extending the system to 4×4-matricies. The Hamiltonian of the system [1]

$$H = v_F\tau_x \otimes \boldsymbol{\sigma}\boldsymbol{k} + m\tau_z \otimes I_2 + bI_2 \otimes \sigma_z + b'\tau_z \otimes \sigma_x, \tag{1.55}$$

with $\boldsymbol{\tau}$ the Pauli matricies related to the pseudospin, and I_2 the identity matrix of dimension 2. The perturbing parameters m, b, b' are a mass parameter, and

Zeeman fields in the z and x direction, respectively. Ignore for now b', i.e. $b' = 0$, which is related to a state known as the line node semimetal. Notice that the b term breaks time reversal symmetry in the system, as the real spin σ is odd under time reversal. The eigenvalues of this system [1]

$$E_{s\mu}(\boldsymbol{k}) = s\left[m^2 + b^2 + v_F^2 k^2 + 2\mu b\sqrt{v_F^2 k_z^2 + m^2}\right]^{\frac{1}{2}}, \tag{1.56}$$

with $s = \pm 1, \mu = \pm 1$ encoding the degeneracies related to the spin and pseudospin degrees of freedom, respectively. There are still linear dispersions for $b > m$. For $b < m$, a gap opens, and the dispersion is non-linear. In fact, this is simply a shift in k_z of the Dirac cone, as is seen by rewriting

$$E_{s\mu}(\boldsymbol{k}) = sv_F\left[k_x^2 + k_y^2 + \left(\sqrt{k_z^2 + \frac{m^2}{v_F^2}} + \mu\frac{b}{v_F}\right)^2\right]^{\frac{1}{2}}. \tag{1.57}$$

This still has Weyl node solutions at $k_z^2 = (b^2 - m^2)/v_F^2$, where the dispersion is linear in the vicinity of the nodal solutions. This thus separates two Dirac nodes in momentum space, giving a *Weyl* semimetal. This also illustrates that the decomposition in Eq. (1.50) is valid around either of the shifted nodes. Expanding around one of the Dirac points of the Weyl semimetal, the Hamiltonian is exactly Eq. (1.50), after decomposing the 4×4 Hamiltonian into its two chiral 2×2 Weyl constituents.

If one instead perturbs the system with a Zeeman field in the x-direction, i.e. having a $b' > 0$, the splitting is instead in energy, giving nodal loop where the two cones intersect. We will not go into any depth on these types of materials.

Possibly rewrite the following sentence

The three cases described here: unperturbed, where the two cones are superimposed; perturbed by b, where the cones are separated in momentum; and perturbed by b', where the cones are separated in energy, are shown in Figure 1.4. Notice that in the two latter cases, the Dirac points, i.e. crossings, are not superimposed. As will be discussed in section 1.6, this makes the crossings very robust, as the two nodes must merge before a gap may be opened.

The Hamiltonian in Eq. (1.50) is not the most general, if we allow for anisotropy in the system. In three dimensions we have more generally the Hamiltonian

$$H(\boldsymbol{k}) = \boldsymbol{v}_0\boldsymbol{k} + (\boldsymbol{v} \odot \boldsymbol{k})\boldsymbol{\sigma}, \tag{1.58}$$

where $\boldsymbol{v}_0$ is the *tilt vector*, $\boldsymbol{v}$ is some, anisotropic velocity, $(\boldsymbol{v} \odot \boldsymbol{k})_i = v_i k_i$ is the Hadamard product of the anisotropic velocity and the momentum, and $\boldsymbol{\sigma}$

are the Pauli matrices corresponding to spin degree of freedom. By a simple rescaling of the momenta, we may in general consider a system with isotropic Fermi velocity v_F, giving

$$H(\boldsymbol{k}) = v_F \boldsymbol{t}\boldsymbol{k} + v_F \boldsymbol{k}\boldsymbol{\sigma}, \tag{1.59}$$

where $\boldsymbol{t}$ is now the (dimensionless) tilt vector. The energy bands are [11]

$$E_s(\boldsymbol{k}) = v_F \boldsymbol{t}\boldsymbol{k} \pm s v_F |k|. \tag{1.60}$$

These types of systems, which are the systems of interest for this thesis, are considered in detail in section 1.6.2.

1.6.1 Chern number of the Weyl point

In order to more explicitly demonstrate the topological nature of the state in Eq. (1.50), we will find a non-zero topological invariant associated with that state. Thereby showing that the material is a topological material. The topological number we will calculate is the Chern number, related to the Berry curvature of the bands in some enclosed surface. In order to calculate the Chern number, we must first find an expression for the Berry curvature of our system. This derivation will follow closely Berry's original derivation [3] of the Berry phase of a two-level system with the Hamiltonian

$$H(\boldsymbol{R}) = \frac{1}{2}\boldsymbol{\sigma}\boldsymbol{R}. \tag{1.61}$$

Some notation has been modernized with inspiration from the treatment of the Berry phase of the spin-1/2 particle in an external magnetic field in Holstein [7].

Suppose we have a Hamiltonian $H(t)$, and that its t-dependence can be parameterized by $\boldsymbol{R} = \boldsymbol{R}(t)$, as in $H(t) = H(\boldsymbol{R}(t))$. Any evolution of the Hamiltonian through time, may then be described as a geometric path through the $\boldsymbol{R}$-space. As the reader might be aware, Berry's most famous discovery was that a closed path through $\boldsymbol{R}$-space gives an observable phase to the system, unlike the non-physical dynamical phase, which may be removed by a suitable choice of gauge. Here we will however focus on the so-called Berry curvature, $\boldsymbol{B}$, a vector field which will be shown to be useful in the categorization of topological materials. Note that there is some variation in the literature on the naming of the various quantities, and the sign convention used. In particular, the word Berry curvature will in some literature refer to a rank two tensor, while our quantity $\boldsymbol{B}$ is referred to as the Berry field strength. In particular, if we let the rank two tensor be denoted F_{ij}, the Berry field strength $\boldsymbol{B}$ is given by

$$B_i = \epsilon_{ijk} F_{jk}. \tag{1.62}$$

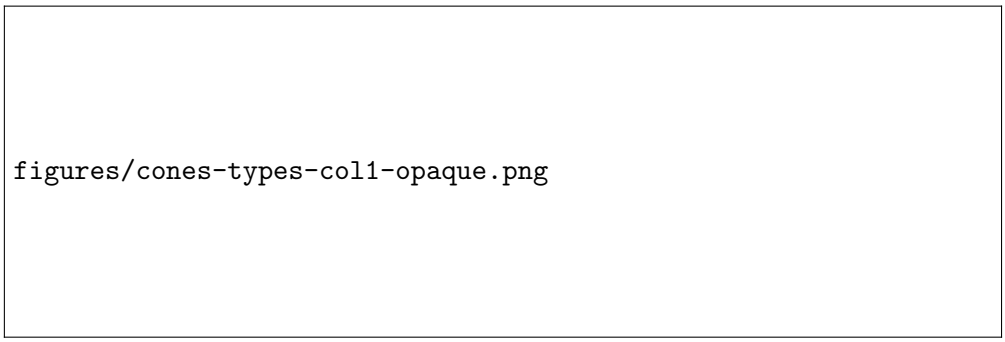

Figure 1.4: Dispersion curves in the k_z, k_x-plane. **(Left)** Dirac material with superimposed cones. **(Center)** Time reversal symmetry broken, giving a Weyl material with the cones separated in momentum space. **(Right)** The cones shifted in energy, givng a nodal loop.

Figure 1.5: Tilted Dirac cones. From left to right the tilt increases, from no tilt in the first cone to overtilt in the last. The three first are Type-I Weyl semimetals, the last is a Type-II semimetal. See main text for details.

Consider rewriting some of this. Look in topology book

The Berry curvature for the state n is explicitly defined as [3]

Should we add some more comments about adabiatic? See topo book

$$\boldsymbol{B_n}(\boldsymbol{R}) = -Im \sum_{m \neq n} \frac{\langle n(\boldsymbol{R})|\nabla_{\boldsymbol{R}} H|m(\boldsymbol{R})\rangle \times \langle m(\boldsymbol{R})|\nabla_{\boldsymbol{R}} H|n(\boldsymbol{R})\rangle}{(E_m(\boldsymbol{R}) - E_n(\boldsymbol{R}))^2}, \tag{1.63}$$

where $\times$ denotes the cross product. Notice that for a degeneracy $E_n = E_m$ there will be an infinity in $\boldsymbol{B_n}$. Considering the Berry curvature as a field in $\boldsymbol{R}$-space, this resembles a source, as will become relevant later. This may now be applied to for example the Weyl semimetal, both in the interest of solidifying the above theory, and as it will be useful in future consideration.

The Hamiltonian around the (untilted) Weyl point is

$$H = v_F \boldsymbol{\sigma} \cdot \boldsymbol{p}, \tag{1.64}$$

with v_F the Fermi velocity, $\boldsymbol{\sigma}$ the Pauli matrices, and $\boldsymbol{p}$ the momentum operator. By letting $\boldsymbol{R} = v_F \boldsymbol{p}$, the Berry curvature of the Hamiltonian can be found. The eigenvalues of this system are

$$E_+ = -E_- = |R|. \tag{1.65}$$

The aforementioned degeneracy is here of course the Weyl point, where $E_+ = E_- = 0$. Noting that

$$\nabla_{\boldsymbol{R}} H = \boldsymbol{\sigma}, \tag{1.66}$$

we can calculate the Berry curvature easily. Denote by $|+\rangle$ the state with the eigenvalue E_+ and $|-\rangle$ the state with the eigenvalue E_-. Take also, without loss of generality, $\boldsymbol{R}$ to be in the z-direction. This gives

$$\boldsymbol{B}_+ = -Im \frac{\langle +|\boldsymbol{\sigma} + v_F \boldsymbol{t}|-\rangle \times \langle -|\boldsymbol{\sigma} + v_F \boldsymbol{t}|+\rangle}{4R^2}. \tag{1.67}$$

As $|+\rangle$ and $|-\rangle$ are eigenstates of σ_z and orthogonal to each other, only the z-component of the cross product may contain non-zero contributions.

$$\begin{aligned} \boldsymbol{B}_+ &= -\frac{\hat{z}}{4R^2} Im \left(\langle +|\sigma_x|-\rangle \langle -|\sigma_y|+\rangle - \langle +|\sigma_y|-\rangle \langle -|\sigma_x|+\rangle \right) \\ &= -\frac{\hat{z}}{2\boldsymbol{R}^2}. \end{aligned} \tag{1.68}$$

Here, the effect of the Pauli matrices on the eigenvectors was used, according to

$$\sigma_x |\pm\rangle = |\mp\rangle \tag{1.69}$$
$$\sigma_y |\pm\rangle = \pm i |\mp\rangle \tag{1.70}$$

Returning to general axis orientations, one has

$$B_+ = -\hat{R}/2\boldsymbol{R}^2 = -\boldsymbol{R}/2\boldsymbol{R}^3. \tag{1.71}$$

For the $|+\rangle$-band, the Weyl point thus takes the form of a negative monopole in R-space; this motivates the requirement that Weyl points must always appear in pairs of opposite chirality, as the divergence of the Berry curvature must always be zero over the entire sample.

There should probably be some care taken here with the sign of v_F.

Extending the calculation to a tilted Weyl cone

$$H = v_F \boldsymbol{\sigma} \cdot \boldsymbol{p} + v_F \boldsymbol{t} \cdot \boldsymbol{p}, \tag{1.72}$$

is trivial. The energies gain a factor $v_F \boldsymbol{t} \cdot \boldsymbol{p} = \boldsymbol{t} \cdot \boldsymbol{R}$, however, this does not change the difference between the energies of the states. Furthermore, the gradient of the Hamiltonian, Eq. (1.66), gains a factor

$$\nabla_{\boldsymbol{R}} H = \boldsymbol{\sigma} + \boldsymbol{t}, \tag{1.73}$$

which does not affect the result, as $\langle \pm | \boldsymbol{t} | \mp \rangle = 0$.

As mentioned, the Chern number is one of several numbers that is used to classify topological materials. The Chern number is defined as

$$C = \frac{1}{2\pi} \oint_{\partial C} \boldsymbol{B}_+ \cdot \mathrm{d}\boldsymbol{S}, \tag{1.74}$$

where the integral is taken over the closed surface ∂C, enclosing the volume C. Noting that the Berry curvature has the shape of a monopole source at $\boldsymbol{p} = 0$, we immediately know the value of this quantity from electromagnetism. We will, however, carry out the computation explicitly here. With the divergence theorem in mind, it behooves us to find the divergence of the Berry curvature. This divergence is zero everywhere except in the monopole source, giving

$$\nabla \cdot \boldsymbol{B}_+ = -\frac{1}{2} \nabla \cdot \hat{R}/R^2 = -2\pi\delta(\boldsymbol{p}), \tag{1.75}$$

where δ is the Dirac delta distribution. By virtue of the divergence theorem the Chern number is then found to be

$$C = \frac{1}{2\pi} \int_C \nabla \cdot \boldsymbol{B}_+ \mathrm{d}C = -1, \tag{1.76}$$

where the property of integrals over Dirac delta distributions was used.

Note that some literature will have a Chern number differing from (1.76) by the sign of the Fermi velocity,

$$C = -\operatorname{sign}(v_F). \tag{1.77}$$

This simply comes from the definition of the eigenstates. We have put the sign dependence in the state, making the E_+ state always have positive eigenenergy. In literature that instead defines $E_+ = v_F|R|$ the state's energy will depend on the sign of the Fermi velocity, and as a consequence, the sign dependence will end up in the Chern number instead.

The overall divergence of Berry curvature must be zero, or equivalently, the sum of the Chern numbers must be zero. The Hamiltonian Eq. (1.61) chosen with the opposite chirality,

$$H(\boldsymbol{R}) = -\frac{1}{2}\boldsymbol{\sigma}\boldsymbol{R}, \tag{1.78}$$

has the opposite Berry curvature, and also the opposite Chern number. Thus, Dirac cones must appear in pairs of opposite chirality, either superimposed as the Dirac semimetal case or separated in momentum space, as the Weyl semimetal.

Make sure there is no discrepancy between 2D/3D materials above

In light of the interpretation of the Dirac point as a monopole of Berry curvature, the discussion in section 1.6, on page 14, on the stability of the band crossing in two and three dimensions gets an intuitive and geometric interpretation. In Figure 1.6 the Berry curvature pole is shown in p-space, together with a plane parallel to the xy-plane, which we will denote the *state plane*. In the two-dimensional case, the state is confined to the state plane, with the z-position of the plane given by any mass terms $m\sigma_z$. In the three-dimensional case, the state is not confined to this plane, as the parameter p_z is a free variable, or alternatively it may be considered as a freedom to move the state plane freely, with its initial position simply shifted by any mass terms. It is thus obvious that one may never reach the monopole in the two-dimensional case, and thus for no $\boldsymbol{k}$ is there a band crossing. Importantly, the Berry curvature is indeed non-zero, however any closed curve of integration will give a Chern number of zero; the monopole has been moved outside the dimensionality of freedom.

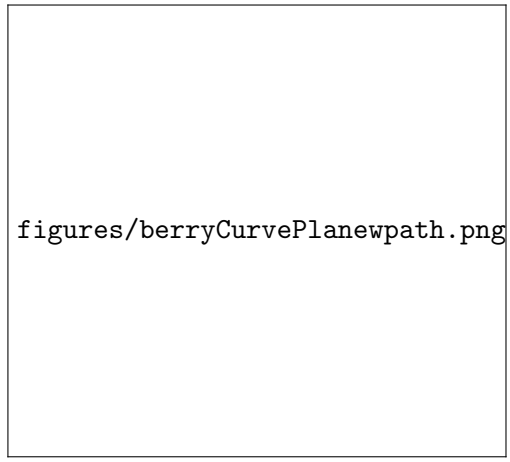

Figure 1.6: The state plane, transparent yellow, parallel to the xy-plane and a Berry curvature monopole at the origin. An integration contour is shown in blue dashed. See main text for details.

1.6.2 Tilted Dirac semimetals – Type-I and Type-II

The conic section problem with the intersecting plane restricted to pass through the node of the cone is trivially seen to have two solutions: a point and two intersecting lines. See figure 1.7. Despite this, the possibility of a Weyl cone tilted beyond the Fermi level was never considered before Soluyanov et al. described this new class of Weyl semimetals in 2015. This now seemingly obvious possibility made an already rich field even more exciting, opening up for a wider range of novel and interesting effects.

add some concrete examples or cites

Is this correct? Is a tilt at all possible in HEP?

In the case of massless fermions, the particle physics equivalent of the Weyl semimetal, such a tilt is not possible, due to the requirement of Lorentz invariance

add cite or explain

. In condensed matter physics, however, this is not an issue, and it is indeed a real class of materials

cite examples

. We denote these types of materials Type-II Weyl semimetals, as opposed to Type-I. The transition between Type-I and Type-II is abrupt – the Fermi

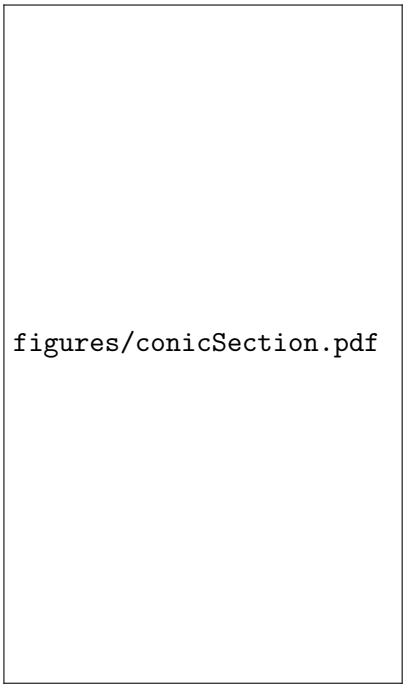

Figure 1.7: Sketch of the conic section with the plane passing through the node of the cone. The intersection surface is either a point at the node or two intersecting lines.

surface goes from a single point to two intersecting lines, in other words going from a zero dimensional to a one dimensional surface.

Make sure this is indeed a one dimensional surface. It is kind of 1DxZ(2)

Make sure it is one dim also for the 3D case, quadric surface, not conic intersection

Type-II also has electron and particle pockets at the Fermi level. While the density of states for a Type-I semimetal goes to zero as one approaches the Fermi level, this causes Type-II to have a finite density of states at the Fermi level.

End with something like: all in all this gives type ii weyl semimetal manifestly different properties from tyep i, useful both in practical applications and as an interesting phenomena seen from a purely scientific perspective

Linear Dirac equation from tight binding model

We will firstly consider a slightly more realistic toy model for a Weyl semimetal, with a parameter taking the system from a Type-I to a Type-II. This is instructive both in order to more intuitively see the origin of the terms causing the tilting of the Dirac cone, and also to see how two Dirac cones in the same Brillouin zone tilt in relation to each other. We will then continue by linearizing the model around the Weyl points, regaining the familiar form of a Dirac cone, with an additional anisotropy term causing the tilt.

Using the general time-reversal breaking model described by McCormick, Kimchi, and Trivedi [10]

$$\begin{aligned} H(\boldsymbol{k}) = &[(\cos k_x + \cos k_z - 2)m + 2t(\cos k_x - \cos k_0)]\,\sigma_1 \\ &- 2t \sin k_y \sigma_2 - 2t \sin k_z \sigma_3 + \gamma(\cos k_x - \cos k_0). \end{aligned} \tag{1.79}$$

The model has Weyl nodes at $\boldsymbol{K}' = (\pm k_0, 0, 0)$, and the parameter γ controls the tilting of the emerging cones. A value of $\gamma = 0$ gives no tilt, while for $\gamma > |2t|$ the Type-II system emerges. Figure 1.8 shows the cross section $k_y = 0$ of the eigenvalues of this system, as γ is gradually increased from 0 to 0.15

verify numbers

. The γ-term "warps" the bands, and in the limit of Type-II the hole band crosses the Fermi level into positive energy, while the particle band crosses the Fermi level into negative energies. We call these hole and electron pockets, respectively.

Linearizing around the Weyl nodes reduces to the familiar expression of a Dirac cone

$$H(\boldsymbol{K}'^{\pm} + \boldsymbol{k}) \approx \mp 2tk_x \sin k_0 \sigma_1 - 2t(k_y\sigma_2 + k_z\sigma_3) \mp \gamma k_x \sin k_0 \sigma_0, \quad k_x, k_y, k_z \ll 1. \tag{1.80}$$

When the separation between the two nodes is π, i.e. $k_0 = \pi/2$, the linearized Hamiltonian of around the cone, is

$$H'(\boldsymbol{k}) = \mp 2tk_x\sigma_x - 2tk_y\sigma_y - 2tk_z\sigma_z \mp \gamma k_x. \tag{1.81}$$

However, as the two noes are brought closer together, the effective Fermi velocity in the x-direction is rescaled, and the system is anisotropic even for no tilt ($\gamma = 0$). The expression may be made even more clear by moving the sign $\pm$-sign into the tilt parameter γ. The Hamiltonian is invariant under a sign change of the first term, as the isotropic Dirac Hamiltonian is invariant under inversion.

Is this not quite jalla?

In the tilt-term, we move the sign dependence into γ, and the linearized model is

$$H'(\boldsymbol{k}) = -2t\boldsymbol{k}\boldsymbol{\sigma} - \gamma^{\pm}k_x, \tag{1.82}$$

where $\gamma^{\pm} = \pm\gamma$ with the upper sign corresponding to the node at $k_x = +k_0$ and the lower sign corresponds to the node at $k_x = -k_0$. As expected, we get two Dirac cones, tilting in opposite direction, but with the same amount.

How does this affect the Berry curvature and chern number?

Maybe prettier/more correct to invert ky and kz, as that would also give the opposite chirality of the dirac points

The linearized model are accurate in describing low energy interactions around the Fermi level. For higher energies their validity falls apart, and more complex models are warranted. In our calculations the linear models is sufficient, and much easier to work with, and we will thus mainly consider the linear model from here on.

The tilt term – symmetries and Type-I vs. Type-II

For tilted Dirac cones we will consider the Hamiltonian

$$H = sv_F\boldsymbol{k}\boldsymbol{\sigma} + v_F\boldsymbol{t}^s\boldsymbol{k}, \tag{1.83}$$

where s denotes the chirality of the Dirac cone, v_F is the Fermi velocity, and $\boldsymbol{t}$ is the *tilt vector*. In general the Fermi velocity is anisotropic, as was the case in the general Dirac Hamiltonian given in Eq. (1.58). By an anisotropic scaling of the momenta $\boldsymbol{k}$, the system may always be mapped to an isotropic case, which we will consider here.

The tilt vector will in general depend on the chirality of the Dirac cone. As the Dirac cones always appear in pairs, $\boldsymbol{t}^s = s\boldsymbol{t}$ will give a system with inversion symmetry. In the case of broken inversion symmetry, we will consider the case of a tilt equal in direction and magnitude between the two cones, $\boldsymbol{t}^s = \boldsymbol{t}$. In short, we define

$$\boldsymbol{t}^s = \begin{cases} \boldsymbol{t} & \text{broken inversion symmetry,} \\ s\boldsymbol{t} & \text{inversion symmetry.} \end{cases} \tag{1.84}$$

This convention is used in most literature [15; 6].

With no magnetic field, the eigenvalues of the system are

$$E(\boldsymbol{k}) = \boldsymbol{\omega_0}\boldsymbol{k} \pm \sqrt{(v_ik_i)^2} = \sqrt{(t_iv_ik_i)^2} \pm \sqrt{(v_ik_i)^2}, \tag{1.85}$$

where in the literature the first term is sometimes referred to as the *kinetic* term while the latter is the *potential* term. The definition for the system to be Type-II is that there exists a direction in momentum space for which the kinetic term dominates over the potential term [14]. The $\boldsymbol{t}$-vector is thus a convenient tool for categorization – if $t > 1$ we have a Type-II, else we have a Type-I.

Proof: We may always rotate our coordinate system such that, without loss of generality, $\boldsymbol{t} = t\hat{x}$. In that case, the first term obviously dominates in the x-direction, when $t > 1$. □

- gives rise to cones tilting opposite direction
- Linearized model valid for low energy interaction. For higher energy, the perfect cone model is not valid, as the cones does in fact touch.
- In this model, the hole pocket is "shared" between the two cones. There are also models with individual pockets (see [10])

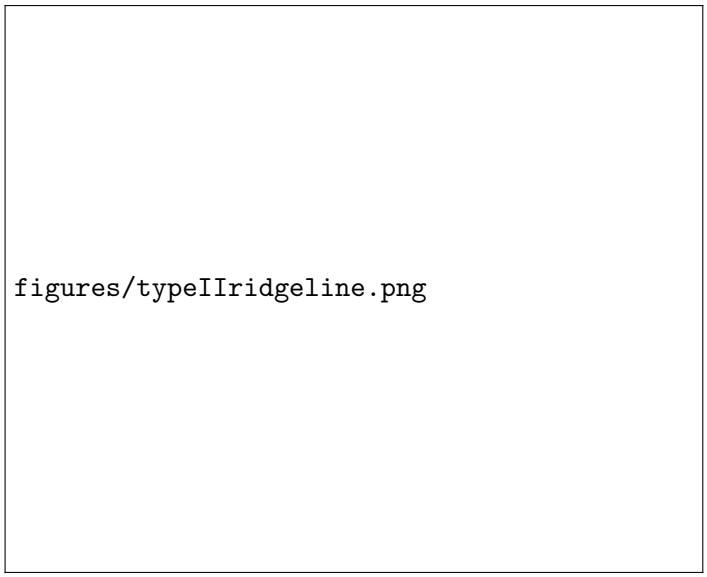

Figure 1.8:

Write this

The values of the parameters were chosen to be $m = 0.15, t = -0.05$, and $2k_0 = \pi$.

Figure 1.9: A Type-II Weyl semimetal with separation between the nodes $2k_0 = 0, \pi/2, \pi$. See main text for details about the model.

Bibliography

[1] N. P. Armitage, E. J. Mele, and Ashvin Vishwanath. "Weyl and Dirac Semimetals in Three-Dimensional Solids". In: *Rev. Mod. Phys.* 90.1 (Jan. 22, 2018), p. 015001. DOI: 10.1103/RevModPhys.90.015001. URL: https://link.aps.org/doi/10.1103/RevModPhys.90.015001 (visited on 09/15/2021).

[2] B. Andrei Bernevig and Taylor L. Hughes. *Topological Insulators and Topological Superconductors*. Princeton: Princeton University Press, 2013. 247 pp. ISBN: 978-0-691-15175-5.

[3] M. Berry. "Quantal Phase Factors Accompanying Adiabatic Changes". In: *Proceedings of the Royal Society of London. A. Mathematical and Physical Sciences* (1984). DOI: 10.1098/rspa.1984.0023.

[4] Maxim N. Chernodub et al. "Thermal Transport, Geometry, and Anomalies". Oct. 11, 2021. arXiv: 2110.05471 [cond-mat, physics:hep-th]. URL: http://arxiv.org/abs/2110.05471 (visited on 10/22/2021).

[5] Hans-Andreas Engel, Emmanuel I. Rashba, and Bertrand I. Halperin. "Theory of Spin Hall Effects in Semiconductors". May 23, 2007. arXiv: cond-mat/0603306. URL: http://arxiv.org/abs/cond-mat/0603306 (visited on 09/20/2021).

[6] Yago Ferreiros, A. A. Zyuzin, and Jens H. Bardarson. "Anomalous Nernst and Thermal Hall Effects in Tilted Weyl Semimetals". In: *Phys. Rev. B* 96.11 (Sept. 8, 2017), p. 115202. DOI: 10.1103/PhysRevB.96.115202. URL: https://link.aps.org/doi/10.1103/PhysRevB.96.115202 (visited on 05/02/2022).

[7] Barry R. Holstein. "The Adiabatic Theorem and Berry's Phase". In: *American Journal of Physics* 57.12 (Dec. 1, 1989), pp. 1079–1084. ISSN: 0002-9505. DOI: 10.1119/1.15793. URL: https://aapt.scitation.org/doi/10.1119/1.15793 (visited on 09/16/2021).

[8] L. D. Landau. "The Theory of a Fermi Liquid". In: *Zh. Eksp. Teor. Fiz.* 30.6 (1956), p. 1058.

[9] A. Manchon et al. "New Perspectives for Rashba Spin–Orbit Coupling". In: *Nature Mater* 14.9 (9 Sept. 2015), pp. 871–882. ISSN: 1476-4660. DOI: 10.1038/nmat4360. URL: https://www.nature.com/articles/nmat4360 (visited on 12/18/2021).

[10] Timothy M. McCormick, Itamar Kimchi, and Nandini Trivedi. "Minimal Models for Topological Weyl Semimetals". In: *Phys. Rev. B* 95.7 (Feb. 21, 2017), p. 075133. DOI: 10.1103/PhysRevB.95.075133. URL: https://link.aps.org/doi/10.1103/PhysRevB.95.075133 (visited on 02/08/2022).

[11] Herman Lileng Ottesen. "Optical Conductivity of Dirac Fermions in Antiferromagnetic Semimetals". Trondheim, Norway: NTNU, June 2021.

[12] Revaz Ramazashvili. "Zeeman Spin-Orbit Coupling in Antiferromagnetic Conductors". In: *Journal of Physics and Chemistry of Solids*. Spin-Orbit Coupled Materials 128 (May 1, 2019), pp. 65–74. ISSN: 0022-3697. DOI: 10.1016/j.jpcs.2018.09.033. URL: https://www.sciencedirect.com/science/article/pii/S0022369718304906 (visited on 09/24/2021).

[13] Jun John Sakurai and Jim Napolitano. *Modern Quantum Mechanics*. 2nd ed. Cambridge: Cambridge university press, 2017. ISBN: 978-1-108-42241-3.

[14] Alexey A. Soluyanov et al. "Type-II Weyl Semimetals". In: *Nature* 527.7579 (7579 Nov. 2015), pp. 495–498. ISSN: 1476-4687. DOI: 10.1038/nature15768 URL: https://www.nature.com/articles/nature15768 (visited on 01/24/2022).

[15] E. C. I. van der Wurff and H. T. C. Stoof. "Magnetovortical and Thermoelectric Transport in Tilted Weyl Metals". In: *Phys. Rev. B* 100.4 (July 11, 2019), p. 045114. DOI: 10.1103/PhysRevB.100.045114. URL: https://link.aps.org/doi/10.1103/PhysRevB.100.045114 (visited on 03/04/2022).

[16] Maria A. H. Vozmediano. "Theoretical Physics Colloquium : Geometry and Anomalies in Dirac Matter". Sept. 22, 2021. URL: https://www.youtube.com/watch?v=Zu2Rzd6rkVQ (visited on 06/06/2022).

[17] Kai Wu et al. "Two-Dimensional Giant Tunable Rashba Semiconductors with Two-Atom-Thick Buckled Honeycomb Structure". In: *Nano Letters* 21 (Dec. 24, 2020). DOI: 10.1021/acs.nanolett.0c04429.